ELEKTROTEHNIŠKI VESTNIK 90(4): 176-182, 2023
ORIGINAL SCIENTIFIC PAPER

Contribution to the calculation of iron losses in Doubly-Salient Switched Reluctance Machine (DSSRM)

Souad Badache[1], Zaki Berrah[2], Omar Hidaoui[3],

Department of Electrical Engineering, Faculty of Electrical Engineering, University of Science and Technology Mohammed Boudiaf, P 1505 – Oran El- M'Naouer 31000 – Algéria
E-mail : badachesouad@yahoo.fr

Abstract. The classical formulations to calculate iron losses at sinusoidal induction cannot be applied to the Doubly Salient Switched Reluctance Machine (DSSRM) because of the polarized induction due to the operating principle. In the literature, there are not many works carried out in this field, and they do not take into account all data needed to evaluate the DSSRM losses. The classical formulations for the sinusoidal induction have been modified to be usable for the non-sinusoidal induction which can have a non-zero mean value as DSSRM. In 1995, Emmanuel HONG who studied modeling and measurement of magnetic losses in douby salient variable reluctance motors developed an analytical formulation to calculate iron losses. This model takes into account the elements of the machine geometric dimensioning control. The analytical calculation using this formulation is very complex and much time consuming and the results may not be accurate. The objective of our work is to develop programs using the Matlab software to simplify the calculation of the iron losses in different parts of DSSRM and to reduce the calculation time. Our programs are easy to use and give results which are more accurate and closer to reality.

Keywords: Doubly-Salient Switched Reluctance Machine (DSSRM), Core losses, iron losses.

Prispevek k izračunu izgub železa v električnem stroju DSSRM

Klasičnih enačb za izračun izgub železa pri sinusni indukciji ni mogoče uporabiti pri električnem stroju DSSRM zaradi polarizirane indukcije. Obstoječe enačbe za sinusoidno indukcijo smo spremenili na način, da so uporabne za nesinusoidno indukcijo. Leta 1995 je Emmanuel Hong, ki je proučeval modeliranje in merjenje magnetnih izgub v motorjih s spremenljivo reluktanco, razvil analitični metodologijo za izračun izgub železa. Analitični izračun z uporabo te formulacije je zelo zapleten in dolgotrajen, zato v prispevku predstavljamo poenostavitev izračuna izgub železa v različnih delih DSSRM ob hkratnem zagotavljanju točnosti izračuna.

1 INTRODUCTION

In the field of electric actuators, the switched reluctance machine has occupied and still occupies very particular slots. Technologically, this machine is simple. The power supply and the excitation windings are placed only in the stator. The rotor has no conductor, its manufacturing cost is low and its robustness considerable allowing to reach high rotation speeds [2, 3]. Its operation above the magnetic saturation region increases its output power [4, 5].

The cost and lifetime of an electric machine are the main aspects that dominate the research. They are directly related to the energy consumption. The energy transformation is often accompanied by various types of losses, ether Joule and mechanical. Controlling the losses is essential to improve the efficiency and thus the performances of an electric machine. Since the losses are dissipated as heat, when not well calculated, the operating temperature is incorrectly evaluated, thus the affecting machine reliability.

For an optimal design of the variable reluctance machine, much work has to be done for electromagnetic optimization [6-10]. Iron losses are sometimes neglected [6,7] or calculated using the classical formulations [8-10] where the magnetic induction is considered to have a sinusoidal form. This is not the case with DSSRM.

In [11-13] the losses are estimated by considering a real case. In [14], the Steinmetz equation was applied to propose an evaluation method using the superposition of the harmonic components of the magnetic induction. Another commonly used approach involves a separation of the hysteresis and eddy current losses [15, 16]. However, some authors [17] claim that the separation has no physical basis and is therefore not reasonable.

Starting from the classical formulations valid for a sinusoidal AC induction and modifying them to be used for the non-sinusoidal induction with a non-zero mean value, the case of DSSRM, are developed new analytical formulations for the calculation of these losses [1]. The developed models take into consideration all the phenomena affecting the machine

Received 4 July 2023
Accepted 9 October 2023

iron losses. Their disadvantage is that they are much consuming time and the results may not be accurate. The problem is how to model sufficient by accurate iron losses in DSSRM with a variable reluctance.

Besides a detailed knowledge of the dissipation phenomena, tools allowing their efficient simulation are also needed. In the paper we present our programs in MATLAB to calculate in a reduced time the DSSRM iron losses in order to get closer to a real case.

2 CLASSIC FORMULATION OF THE IRON LOSSES

The classical formulation to calculate the iron losses in electric machines at a sinusoidal induction (Steinmetz equation) is [18]:

$$P_{fer}(w/kg) = KB_m^{\alpha} f^{\beta}, \quad 1<\alpha<2 \text{ and } 1<\beta<2 \qquad (1)$$

Another formulation separating the hysteresis and eddy current losses is given by:

$$P_{fer}(w/kg) = (K_{h1}B_m + K_{h2}B_m^2)f + K_f B_m^2 f^2 \qquad (2)$$

where :
B_m is the induction amplitude [Tesla] and f is the Induction frequency [Hz].

By testing the samples assembled on standardized measuring frames and subjecting them to sinusoidal inductions of the amplitude and frequency, the value of coefficients K, α, β, K_{h1}, K_{h2} and K_f are determined.

3 DSSRM FORMULATION

In DSSRM, the induction is polarized due to the operation. In an electrical operation, there is a magnetization and demagnetization phase. In general, the degaussing is complete. This means that the induction varies between a zero and a maximum value. Figures 1, 2 and 3 show examples of the induction forms of the switched reluctance machine with a double salience of six stator teeth and four rotor teeth supplied with a full voltage wave. The examples enable realization of the orders of the magnitude of the inductions involved, working frequencies and waveforms.

3.1 Minor cycles

When the induction varies between two extreme values (for example between $-B_m$ and $+B_m$ in the case of an alternative or bipolar induction or between 0 and $+B_m$, in the case of a unipolar induction), the variation may not be monotonous. In such case, a mini hysteresis cycle occurs within the main cycle (Figure 4).
Such minor cycle affects the expression of the hysteresis energy [19].

The contribution of the cycle to the loss term which corresponds to the eddy current losses is considered.

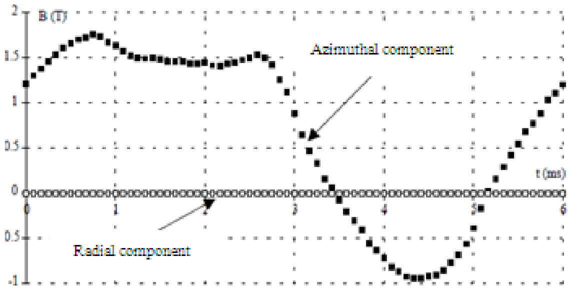

Figure 1. Induction in a zone of the stator yoke of SRM 6/4 at 2500 rpm.

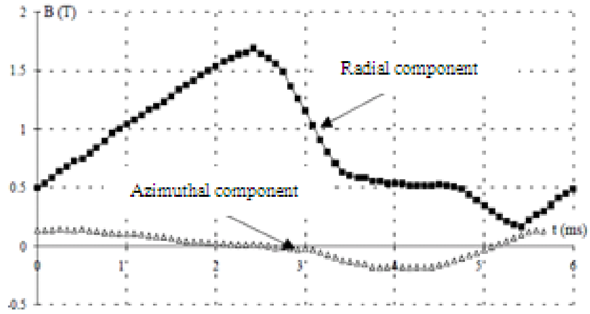

Figure 2. Induction in a zone of the stator teeth of SRM 6/4 at 2500 rpm.

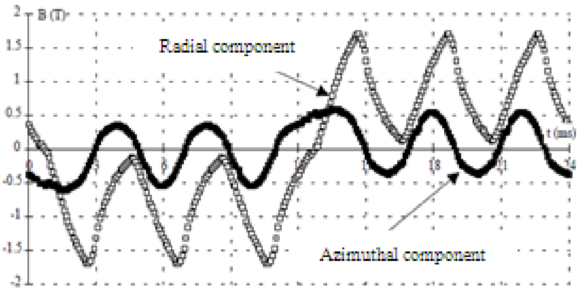

Figure 3. Induction in a zone of the rotor teeth of SRM 6/4 at 2500 rpm.

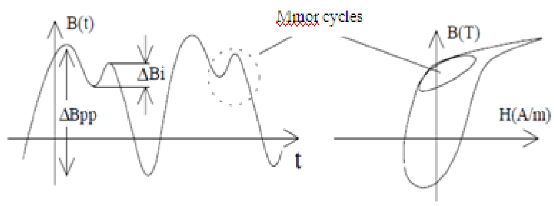

Figure 4. Induction with minor cycles.

The DSSRM takes into account the elements of the machine geometric dimensioning, (Figure 5 for an DSSRM6/4 example), and control. The current or voltage control parameters are the value of the DC voltage at the output of the power supply and the magnetization angle. The formulations for each type of the control are given below.

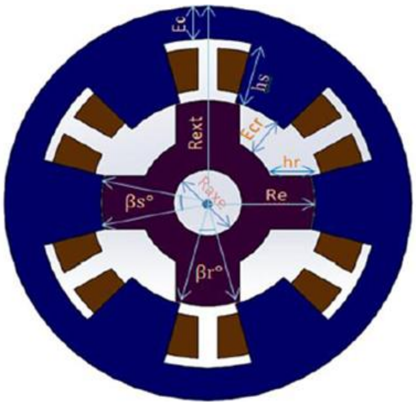

Figure 5. 2D geometry of DSSRM 6/4.

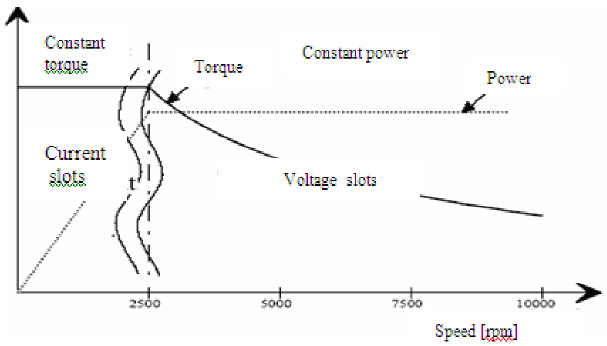

Figure 6. Feeding strategies according to the rotational speed [20].

3.2 *Current pulse control - Iron loss model*

When the rotational speed is lower than the base speed (2500 rpm), the operation is at a constant torque, and the actuator is controlled by current pulses (Figure 6). The pulses are injected during the inductance rise phase for the motor mode operation. The torque is adjusted by adjusting the value of the current pulses. The control with the pulse modulation (PWM) is necessary. To calculate the iron losses, the actuator is divided down into four parts (stator yoke, stator teeth, rotor teeth and rotor yoke). The hypotheses adopted in this case are as follows:

a- Decomposition of the structure into four main parts: a - Stator yoke, b - Stator teeth, c - Rotor teeth, d - Rotor yoke.

b-The flux in the four main parts can be deduced from the forced flux in the windings.

c-The flux is identical throughout the stator yoke. For this, the direction of the windings must be alternated.

d- In each part, there is only one component of the induction vector.

The iron loss model adopted is :

$$P_{fer} = (K_{h1}\Delta B + K_{h2}\Delta B^2)f + \alpha_p \frac{1}{T}\int_0^T \left(\frac{dB(t)}{dt}\right)^2 dt \qquad (3)$$

ΔB: Variation in the flux density [Tesla].

Remarks:

a- The minor cycles in this case are often of a low amplitude; their impact on the iron losses is therefore low.

b- The integral $\frac{1}{T}\int_0^T \left(\frac{dB(t)}{dt}\right)^2 dt$ is named F_2.

The iron losses are dependent on the maximum flux. The hysteresis losses depend on the excursion of the induction. The losses caused by eddy currents, in the control mode, depend only on the supply voltage and not on the flux level. The results for each part are summarized in Table1. W_s, w_r are the widths of the stator and rotor teeth, respectively [mm].

Table1. The calculation of the iron loss densities in the four DSSRM parts.

	ΔB	***f***	**F_2**	**Volume**
Stator yoke	$\frac{\varphi_m}{E_c l_a}$	$f_{elec} = N_r f_{rot}$	$\left(\frac{U}{2n_s E_c l_a}\right)^2$	$\pi\left(R_{ext}^2 - (R_{ext} - E_c)^2\right)l_a$
Stator teeth	$\frac{\varphi_m}{w_s l_a}$	$\frac{1}{2}\frac{N_s}{N_r} f_{elec} = \frac{1}{2} N_s f_{rot}$	$\alpha\left(\frac{U}{n_s w_s l_a}\right)^2$	$N_s h_s w_s l_a$
Rotor teeth	$\frac{\varphi_m}{w_s l_a}$	$f_{elec} = N_r f_{rot}$	$\alpha\frac{N_s}{N_r}\left(\frac{U}{n_s w_r l_a}\right)^2$	$N_r h_r w_r l_a$
Rotor yoke	$\frac{\varphi_m}{E_{cr} l_a}$	$f_{elec} = N_r f_{rot}$	$\left(\frac{U}{2n_s E_{cr} l_a}\right)$	$\pi\left((R_{axe} + E_{cr})^2 - R_{axe}^2\right)l_a$

A program written in MATLAB is developed to determine the iron losses in the different DSSRM parts and in the entire magnetic circuit of the machine. The flowchart in the figure below shows the main programming steps.

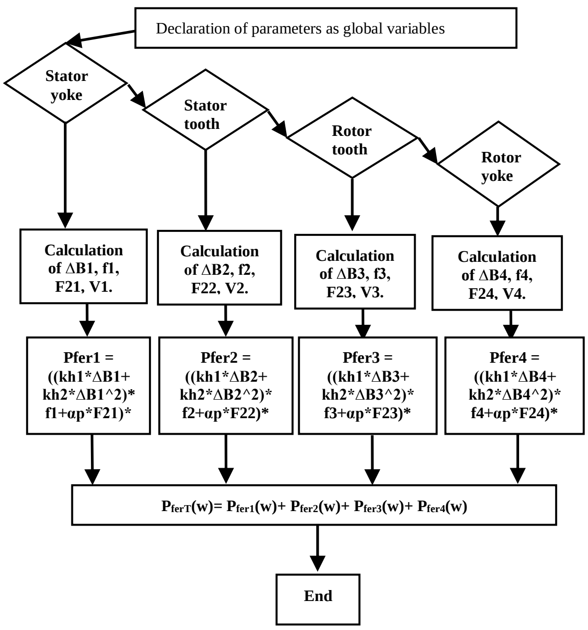

Figure 7. Algorithm to calculate the iron losses in the current pulses control.

3.3 Voltage step control - Iron loss model

In any power system, limits are set by the supply voltage, maximum acceptable current and the temperature rise. [21, 22] show that the mode of powering in current slots is viable only from the energy point of view at a low speed. At a high speed, the operation at a constant power (Figure 6), the supply mode then used is the voltage control. The voltage "seen" by a phase is a square of the height equal to the voltage of the DC power supply (Figure 8). The duration and the position (control parameters) are chosen according to the mechanical (useful torque) and electrical constraints (Joule and iron losses and semiconductors dimensioning).

Hypotheses

a - Voltage supply, the flux is forced. The DC voltage is perfectly filtered.
b - Dividing the structure into four main parts: a - stator yoke b - stator teeth c - rotor teeth d - rotor yoke
c - The flux in the four main parts can be obtained from the forced flux in the windings.
d - At a full voltage wave supply, the angle of the advance does not affect the value of the iron losses.
e - The flux is identical in all parts of the stator yoke.
f - In each part, there is only one component of the induction vector.

The hypothesis (d) is due to the dividing the machine into four parts where it is no longer possible to distinguish the flux variations produced by the variation in the magnetic circuit value. This is interesting only at temporal variations in the induction due to the power supply.

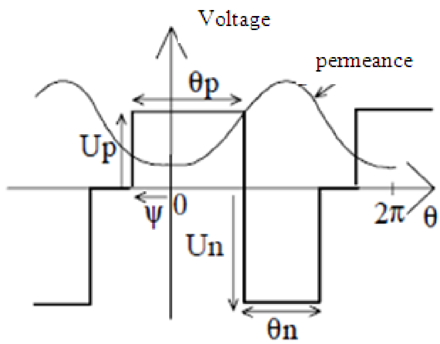

Figure 8. Definition of the command parameters.

U_p is the positive slot height,
U_n is the negative slot height (Usually Un = Up),
Θ_p is the positive slot duration and
Θ_n is the negative slot duration.
With $U_p{*}\Theta_p = U_p{*}\Theta_n$, the degaussing is complete.
ψ is the angle of the advance relative to the opposition position.

Given the above hypotheses, the formulation has as a variable. The vector induction is given by:

$$P_{fer} = (K_{h1}\Delta B + K_{h2}\Delta B^2)f + \alpha_p \frac{1}{T}\int_0^T \left(\frac{dB(t)}{dt}\right)^2 dt + F_4\left(K_{h1}\left(\frac{F_3}{F_4}\right) + K_{h2}\left(\frac{F_3}{F_4}\right)^2\right)f \qquad (4)$$

where F_3 is the sum of the amplitudes of the minor cycles and F_4 is their quantity.

Remarks:
ΔB is the peak-to-peak of the induction,
F_2 is the square of the effective value of the time derivative of the induction,
F_3 is the excursion of the minor cycles end,
F_4 is the number of the minor cycles.
The results for each part are summarized in the following tables:

a- Stator teeth

$$B_m = \frac{U}{n_s w_s l_a}\frac{\theta_p}{\pi}\frac{T}{2}; \quad f = f_{elec} = N_r f_{rot}; \quad volume = N_s h_s w_s l_a$$

Table 2. Iron loss densities in the stator teeth.

Θ_p	ΔB	F_2	F_3	F_4
$0 \le \theta_p \le \pi$	B_m	$\frac{4\pi}{\theta_p} B_m^2 f^2$	0	0

b- Stator yoke

$$B_m = \frac{U}{2n_s E_c l_a}\frac{\theta_p}{\pi}\frac{T}{2}; \quad f = f_{elec} = N_r f_{rot}; \quad volume = \pi\left(R_{ext}^2 - (R_{ext} - E_c)^2\right)l_a$$

Table 3. Iron loss densities in the stator yoke.

Θ_p	ΔB	F_2	F_3	F_4
$\theta_p \le \frac{\pi}{3}$	$2B_m$	$\frac{12\pi}{\theta_p} B_m^2 f^2$	B_m	1
$\frac{\pi}{3} \le \theta_p \le \frac{2\pi}{3}$	$2B_m$	$\left(48 - \frac{36\theta_p}{\pi}\right) B_m^2 f^2$	$\left(2 - \frac{3\theta_p}{\pi}\right) B_m$	1
$\frac{2\pi}{3} \le \theta_p \le \pi$	$B_m\left(\frac{8}{3} - \frac{\theta_p}{\pi}\right)$	$\left(\frac{128}{3} - \frac{28\theta_p}{\pi}\right) B_m^2 f^2$	0	0

c- Rotor teeth

$$B_m = \frac{U}{n_s w_r l_a}\frac{\theta_p}{\pi}\frac{T}{2}; \quad f = \frac{1}{2}\frac{N_s}{N_r} f_{elec} = \frac{1}{2} N_s f_{rot}; \quad volume = N_r h_r w_r l_a$$

Table 4. Iron loss densities in the rotor teeth.

Θ_p	ΔB	F_2	F_3	F_4
$0 \le \theta_p \le \pi$	$2B_m$	$\frac{16\pi}{\theta_p} B_m^2 f^2$	0	0

d- Rotor yoke

$$B_m = \frac{U}{2n_s E_{cr} l_a}\frac{\theta_p}{\pi}\frac{T}{2}; \quad f = f_{elec} = N_r f_{rot}; \quad volume = \pi\left((R_{axe} + E_{cr})^2 - R_{axe}^2\right)l_a$$

The table to calculate ΔB, F_2, F_3 and F_4 is identical to that for the stator yoke.
With the established formulations, the volume losses in the four parts of the actuator are calculated according to the voltage control parameters and geometric dimensions.

3.3.1 Synthetic formulation of the machine iron losses

The formulations can be grouped together to obtain the one valid for the whole machine. This formulation gives the value of the iron losses as a function of the control parameters (supply voltage U and duration of application of voltage θ_P), of the geometric parameters (L_a, E_c, w_s, w_r, n_s etc.) and of the characteristics magnetic strips (k , kh_2, α_P).The total iron losses take the form:

$$P_{fer}(w) = K_1 U + K_2 \frac{U^2}{f} + K_3 U^2 \tag{5}$$

$K_1 = K_1(\theta_p)$, $K_2 = K_2(\theta_p)$, $K_3 = K_3(\theta_p)$

For $\Theta_p \leq \pi/3$

$$K_1 = \frac{k_{h1}}{2}\left(\frac{\theta_p}{n_s\pi}\right)\left[N_s h_s + \frac{3\pi}{2}\left(\frac{R_{ext}^2-(R_{ext}-E_c)^2}{E_c}+\frac{(R_{axe}+E_{cr})^2-R_{axe}^2}{E_{cr}}\right)+N_s h_r\right] \tag{6}$$

$$K_2 = \frac{k_{h2}}{L_a}\left(\frac{\theta_p}{n_s\pi}\right)^2\left[\frac{N_s h_s}{4w_s} + \frac{5\pi}{16}\left(\frac{R_{ext}^2-(R_{ext}-E_c)^2}{E_c^2}+\frac{(R_{axe}+E_{cr})^2-R_{axe}^2}{E_{cr}^2}\right)+\frac{N_s h_r}{2w_r}\right] \tag{7}$$

$$K_3 = \frac{\alpha_p}{n_s^2 L_a}\left(\frac{\theta_p}{\pi}\right)\left[\frac{N_s h_s}{w_s} + \frac{3\pi}{4}\left(\frac{R_{ext}^2-(R_{ext}-E_c)^2}{E_c^2}+\frac{(R_{axe}+E_{cr})^2-R_{axe}^2}{E_{cr}^2}\right)+\frac{N_s^2 h_r}{N_r w_r}\right] \tag{8}$$

For $\pi/3 \leq \Theta_p \leq 2\pi/3$

$$K_1 = \frac{k_{h1}}{2}\left(\frac{\theta_p}{n_s\pi}\right)\left[N_s h_s + \frac{4-\frac{3\theta_p}{\pi}}{2}\pi\left(\frac{R_{ext}^2-(R_{ext}-E_c)^2}{E_c}+\frac{(R_{axe}+E_{cr})^2-R_{axe}^2}{E_{cr}}\right)+N_s h_r\right] \tag{9}$$

$$K_2 = \frac{k_{h2}}{L_a}\left(\frac{\theta_p}{n_s\pi}\right)^2\left[\frac{N_s h_s}{4w_s} + \frac{4+\left(2-\frac{3\theta_p}{\pi}\right)^2}{16}\pi\left(\frac{R_{ext}^2-(R_{ext}-E_c)^2}{E_c^2}+\frac{(R_{axe}+E_{cr})^2-R_{axe}^2}{E_{cr}^2}\right)+\frac{N_s h_r}{2w_r}\right] \tag{10}$$

$$K_3 = \frac{\alpha_p}{n_s^2 L_a}\left(\frac{\theta_p}{\pi}\right)\left[\frac{N_s h_s}{w_s} + \frac{4-\frac{36\theta_p}{\pi}}{16}\theta_p\left(\frac{R_{ext}^2-(R_{ext}-E_c)^2}{E_c^2}+\frac{(R_{axe}+E_{cr})^2-R_{axe}^2}{E_{cr}^2}\right)+\frac{N_s^2 h_r}{N_r w_r}\right] \tag{11}$$

For : $2\pi/3 \leq \Theta_p \leq \pi$

$$K_1 = \frac{k_{h1}}{2}\left(\frac{\theta_p}{n_s\pi}\right)\left[N_s h_s + \frac{\frac{8}{3}-\frac{\theta_p}{\pi}}{2}\pi\left(\frac{R_{ext}^2-(R_{ext}-E_c)^2}{E_c}+\frac{(R_{axe}+E_{cr})^2-R_{axe}^2}{E_{cr}}\right)+N_s h_r\right] \tag{12}$$

$$K_2 = \frac{k_{h2}}{L_a}\left(\frac{\theta_p}{n_s\pi}\right)^2\left[\frac{N_s h_s}{4w_s} + \frac{\left(\frac{8}{3}-\frac{\theta_p}{\pi}\right)^2}{16}\pi\left(\frac{R_{ext}^2-(R_{ext}-E_c)^2}{E_c^2}+\frac{(R_{axe}+E_{cr})^2-R_{axe}^2}{E_{cr}^2}\right)+\frac{N_s h_r}{2w_r}\right] \tag{13}$$

$$K_3 = \frac{\alpha_p}{n_s^2 L_a}\left(\frac{\theta_p}{\pi}\right)\left[\frac{N_s h_s}{w_s} + \frac{\frac{128}{3}-\frac{28\theta_p}{\pi}}{16}\theta_p\left(\frac{R_{ext}^2-(R_{ext}-E_c)^2}{E_c^2}+\frac{(R_{axe}+E_{cr})^2-R_{axe}^2}{E_{cr}^2}\right)+\frac{N_s^2 h_r}{N_r w_r}\right] \tag{14}$$

In expressions K_1, K_2 and K_3, variable θ_P is expressed in radians.

The flowchart below shows the main programming steps.

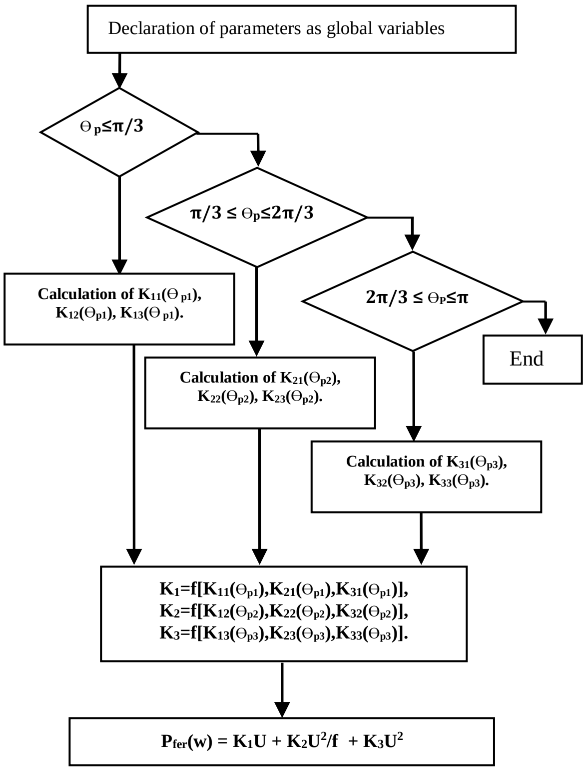

Figure 9. Algorithm to calculate the iron losses for the voltage pulse control.

3.3.2 Results

To validate the presented results, an DSSRM6/4 with the Ns/Nr structure is used: Ns=six poles at the stator and Nr= four poles at the rotor. The actuator operates according to specifications determined for the use in the electric vehicle, the base speed is 2500 rpm. The actuator operates at a constant power from 2500 rpm to 10000 rpm. The angle of the voltage application duration θ_p is set at 105°. The torque to be supplied is 103 Nm and the power is 27 kW. The voltage of the power source is 120 V. The laminations of the magnetic circuit are in Fe-Si (3%) with a thickness of 0.35 mm, hence, the values of the coefficients are: kh_1 = 5, kh_2 = 40 and α_p = 0.022. Figure 5 shows the geometry of the studied machine, Table 5 indicates its dimensions (L_a is the active length of the machine, e is the thickness of the air gap and n_s is the number of turns of the coil).

Figures 10 and 11 present the results obtained for the machine for the current and voltage control, respectively. The iron losses are proportional to the speed. There is a good agreement between the analytical results and those found by the numerical calculation in MATLAB. A slight difference appears between the two results; it is due to the accuracy of the numerical calculation.

Table 5. DSSRM6/4 dimensions.

R_{est}	R_e	R_{axe}	L_a	E_c	h_s	β_s	β_r	h_r	E_{cr}
125	65	21	150	20.5	38.5	30	35.1	23	21

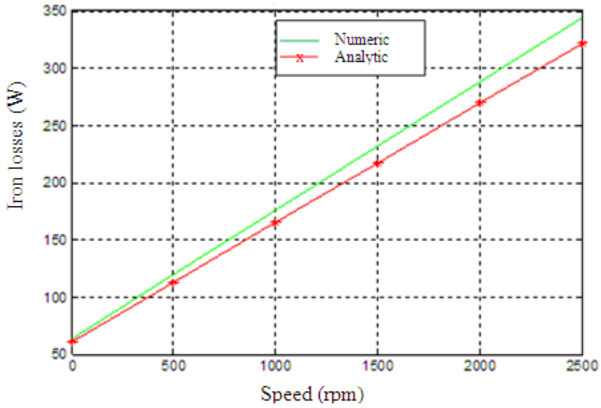

Figure 10. Total iron losses as a function of the speed for the control in current pulses.

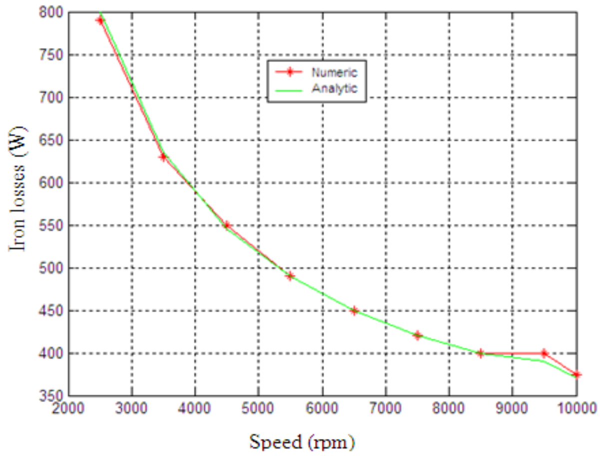

Figure 11. Total iron losses as a function of the speed for the voltage pulse control.

4 Conclusion

The paper calculates iron losses in adoubly-salient switched reluctance machine (DSSRM). For conventional electric machines, classic formulations are used taking into account the shape of the sinusoidal induction. The case is not the same with DSSRM. The investigated models are simple and are derived from classical models taking into account the hysteresis and eddy currents losses. A detailed study of the machine iron losses shows the difference with other conventional machines. Speaking in terms of accuracy, calculation time and exploitation of the results, a choice must be made between using either analytical or numerical calculation method. As the analytical calculation is very complex and much time-consuming, the steps taken to calculate the losses using the MATLAB software are presented. The results show that the developed programs are very perform satisfactorily and can be used to calculate the efficiency of the investigated machines and they enable a correct thermal analysis of the machine magnetic circuits.

References

[1] E.Hoang “Etude, Modélisation et mesure des pertes magnétiques dans les moteurs à reluctance variable à double saillance”, *thesis from the normal higher school of cachan, France, December 1995*.

[2] J. Faiz, G. Soltani-Khosroshani, “Torque ripple minimization in switched reluctance motor optimal commutation strategy using a novel reference torque”, *Journal of Electric Power Components and Systems, 2002, pp. 769–782.*

[3] J. Faiz, J.W. Finch, “ Aspects of design optimization for switched reluctance motors ”, *IEEE Transactions on Energy Conversion, 1993, pp. 704–713.*

[4] P.J. Lawrenson, J.M. Stephenson, P.T. Blenkinsop, J. Corda, N.N. Fulton, “Variable-speed switched reluctance motor”, *IEE Proceedings Part B 127, 1980, pp. 253–265.*

[5] W. Wu, J.B. Dunlop, S.J. Collocott, B.A. Kalan, “Design optimization of a switched reluctance motor by electromagnetic and thermal finite element analysis”, *IEEE Transactions on Magnetics , 2003, pp. 3334–3336.*

[6] K.N.Srinivas, R.Armugam**,** “Analysis and characterization of switched reluctance motors: part II-flow, thermal and vibration analysis”, *IEEE transaction on magnétique, 2005*

[7] J.M.Ojeda, “Dimensionnement et commande d’actionneurs piézoélectriques en vue de contrôle des vibrations des machines à reluctance variable rapides”, PhD thesis *from the normal school of Cachan, France,* june 2009.

[8] S.Inamura, T.Sakai, K.Sawa, ”A temperature rise analysis of switched reluctance motor due, to the core and copper loss by FEM”, *IEEE, June 2002*.

[9] S. Shoujun, L. Welguo, D. Peitsch, U. Schaefer, “Detailed Design of a High Speed Switched Reluctance Starter/Generator for More/All Electric Aircraft”, *Science Direct, Chinese Journal of Aeronautics, 2009.*

[10] L. Guang-Jin, “Contribution à la Conception des Machines Electriques à Rotor Passif pour des Applications Critiques : Modélisations Electromagnétiques et Thermiques sur Cycle de Fonctionnement, Etude du Fonctionnement en Mode Dégradé”, PhD thesis *from the normal school of Cachan, France*, July 2011.

[11] A. Matveev, “Development of methods, algorithms and software for optimal design of switched reluctance drives”, *PhD thesis, Thechnische Universiteit Eindhoven, 2006*.

[12] H.Rouhani, J. Faiz, C. Lucas, “Lumped thermal model for switched reluctance motor applied to mechanical design optimization”, *Science Direct, Mathematical and Computer Modeling, 2007.*

[13] S.Badache, A.Taieb Brahimi, “Thermal phenomena analysis of 6/4 switched reluctance machine by the 2D finite elements method”, *In: Journal of Electrical Engineering, volume13, Edition 3, 2013.*

[14] P. N. Materu, R. Krishnan, ”Estimation of switched reluctance motor losses”, *IEEE Trans. on Industry Applications, 28(3):668-679, May/June 1992.*

[15] Y. Hayashi, T.J.E. Miller, “A new approach to calculating core losses in SRM”, *IEEE Trans. on Industry Applications, 31(5):1039-1046, September/October 1995*.

[16] M. Turner, “Switched reluctance drives: Technology, applications, operation & performance”, *Motor, Drive & Automation Systems Conference, Orlando, Florida, 2009.*
[17] J. Reinert, A. Brockmeyer, R.W. DE Doncker, “Calculation of losses in ferro-and ferrimagnetic materials based on the modified Steinmetz equation”, *IEEE Trans. on Industry Applications, 37(4):1055-1061, July/August 2001.*
[18] C. P. Steinmetz, “On the law of hysteresis”, *Proceedings of the IEEE , vol. 72, no. 2, pp. 197–221, Feb, 1984.*
[19] A. Kedous-Lebouk, “Electromagnétisme et matériaux magnétiques pour le génie électrique”, *ENSIEG-2èmeNRJ-2005/2006.*
[20] S. Mouellef**, «** Contribution à l’étude d’une machine à reluctance variable: Conception, modélisation et simulation d’une MRV6/4”, *Memory of Magister of the University of Mentouri of Constantine, Algeria, June 2008.*
[21] H.B. Ertan, O.F. Yagan, A. Diriker, “Optimum parameters for doubly-salient motors driven by a voltage source drive”, *ICEM 90, vol. 3, pp 806-811, 1990*.
[22] H.H. Moghbelli, M.H. Rashid, “The switched reluctance motor drives : characteristics and performances”, *EPE Firenze, pp 1-398 1-403,1991.*

Souad Badache received her B.Sc., M.Sc. and Ph.D. degrees in 1996, 2005 and 2015 respectively, from the Electrical Engineering Institute of the University of Sciences and Technology of Oran (USTO). She is currently a Professor of Electrical Engineering at The same. Her research interest is in heat transfer in electric machines.

Zaki Berrah is a student at the University of USTO. He received his M.Sc degree in Electrical Engineering in 2017 from the University of USTO, Oran. His research interest is in heat sources and heat transfer in electric machines.

Omar Hidaoui received his M.Sc degree in Electrical Engineering in 2020 from the University of USTO, Oran. His research interest is in heat sources and heat transfer in electric machines.